Structural Engineering and Mechanics, Vol.2, No.1 (1994) 95-112
DOI: http://dx.doi.org/10.12989/sem.1994.2.1.095

Modelling the dynamic response of railway track to wheel/rail impact loading

Z.Cai †

Department of Civil Engineering, Royal Military College, Kingston, Ontario, Canada, K7K 5L0

G.P. Raymond ‡

Department of Civil Engineering, Queen's University, Kingston, Ontario, Canada, K7L 3N6

Abstract. This paper describes the formulation and application of a dynamic model for a conventional rail track subjected to arbitary loading functions that simulate wheel/rail impact forces. The rail track is idealized as a periodic elastically coupled beam system resting on a Winkler foundation. Modal parameters of the track structure are first obtained from the natural vibration characteristics of the beam system, which is discretized into a periodic assembly of a specially-constructed track element and a single beam element characterized by their exact dynamic stiffness matrices. An equivalent frequency-dependent spring coefficient representing the resilient, flexural and inertial characteristics of the rail support components is introduced to reduce the degrees of freedom of the track element. The forced vibration equations of motion of the track subjected to a series of loading functions are then formulated by using beam bending theories and are reduced to second order ordinary differential equations through the use of mode summation with non-proportional modal damping. Numerical examples for the dynamic responses of a typical track are presented, and the solutions resulting from different rail/tie beam theories are compared.

Key words: railway track; dynamics; impact loading; modal analysis.

1. Introduction

The structural configuration of a conventional railway track appears to be relatively simple: two parallel rail beams resting on regularly spaced cross-track ties through elastic fastening mechanisms and/or resilient pads. The dynamic analysis of the track system, however, is a considerably difficult subject. Conventional studies of rail track dynamics simplified the interconnected track/beam system as merely a Bernoulli-Euler type beam(rail) on an elastic (Winkler type) foundation, or BOEF (Kenney 1954, Fryba 1972, Kerr 1972, Patil 1988, Duffy 1990). Research on the vibration of periodic multi-span beams on discrete elastic supports, which may be used to approximate rail track structures has been reported extensively in the literature (Mead and Yaman 1991, Lewandowski 1991, Munjal and Heckl 1982). The use-

† Research Associate
‡ Professor

fulness of these methods in dealing with general railway track dynamics is limited since they usually consider simple regular loading patterns characterized by a point harmonic force. Dynamic forces on a conventional railway track caused by abnormal wheel/rail impacts due to, for example, wheel flats, rail joints, etc., are usually highly impulsive with short durations and high frequency components. Solutions that are of interest to a track engineer, such as dynamic rail stresses/strains, rail seat forces, and stresses/strains in the ballast/subgrade, cannot be readily obtained from these approaches. Furthermore, these methods do not consider the case where a transverse member acts, through elastic coupling elements, as a flexural sub-component supporting the beam, such as a cross-track tie (both the flexural and inertial effect) in the rail track/beam system. The discrete nature of the rail support sub-components and the flexural effects of the tie beams have been included in track modelling by only a limited number of authors (Ono and Yamada 1989, Clark et al. 1982, Grassie and Cox 1984) where only the Bernoulli–Euler theory may be used to describe the rail. The Timoshenko beam theory has previously been used to describe the rail only when the track substructure components are modelled as a continuous layer(s) of elastic foundation (Grassie 1984).

This paper presents an improved method to model the track/beam system where all the track components are more realistically represented and the applied loading function can be arbitrary. Both the Timoshenko beam theory and the Bernoulli–Euler (or simple) beam theory can be used to describe the rail/tie structures as flexible beams while the rail is discretely coupled to the ties. The physical modelling technique adopted herein follows a similar but modified procedure to that used by Clark et al. 1982, who represented the rail/tie members as Bernoulli–Euler type beams with proportional modal damping subjected to a single mass/spring system as the excitation source. The excitation input considered in the present study, however, consists of a single or a series of deterministic forcing functions representing dynamic wheel/rail impact loads.

Although the track in reality is subjected to moving wheel loads, the use of a deterministic stationary impact function as an excitation source to the track system nevertheless provides valuable insight into the characteristics of rail track dynamic responses under wheel/rail impact loading. For example, a wheel flat or a rail joint creates a distinct wheel/rail impact force with a short duration which can be described by a given force–time relationship. It has particular application in evaluating existing static methods (AREA 1991) for analyzing track responses under a pseudo-dynamic force (which is equal to the static wheel load multiplied by an empirical dynamic factor). This has been demonstrated by the frequent use of drop-weight tests where sharp impact force is produced by a weight falling on the rail to simulate wheel/rail impact loads (Igwemezie et al. 1993, Scott and Charenko 1985, Dean et al. 1982, Cannon and Sharpe 1981). The moving dynamic wheel/rail interaction problem belongs to a different category of rail track dynamics and has been addressed elsewhere (Raymond and Cai 1993, Cai and Raymond 1992).

2. Model description

The idealized rail track/beam system is illustrated in Fig. 1. The vertical dynamic track model considers a conventional ballasted tie track where both the rail and the tie may be described by either the Bernoulli–Euler beam theory, or the Timoshenko beam theory. The rail beam is assumed to be periodically coupled at discrete points to the cross-track tie beams

through the coupling spring/damper elements representing the resilience and damping of the rail pads and rail–fastening mechanisms. In addition, an axial force in the rail beam is included to simulate thermal forces. To consider concrete tie beams that have deeper shoulder sections, the tie beam can be non–uniform as shown in Fig. 1.b. The distributed spring/damper constants beneath each tie represent the elasticity and damping effect of the track foundation (ballast and subgrade). To account for uneven ballast/subgrade compaction efforts across the track, the distributed stiffness/damping coefficient beneath the center portion of the tie beam may be assumed to be different from (always lower than) that beneath the two end segments of the tie.

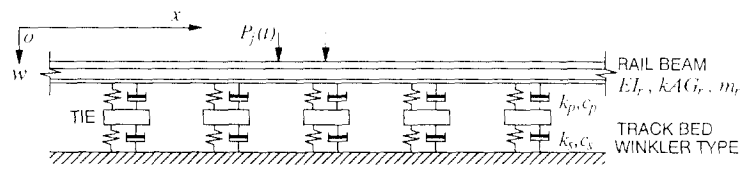

(a) Longitudinal view

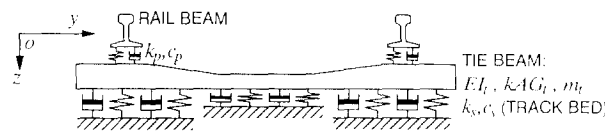

(b) Transverse(CROSS–TRACK) view

Fig. 1 Idealized Vertical Rail Track Vibration Model

3. Natural vibration analysis of track/beam system

3.1. Formulation of generalized track element

One distinct structural feature of a rail track is its periodic chain–type configuration. To obtain solutions to the fundamental vibration characteristics of the track model shown in Fig. 1, a generalized track element, as illustrated in Fig. 2.a, is devised. It is an assembly of a rail span and the two corresponding substructure units that include the rail/tie contact stiffness elements (rail pads+rail fastening units), two adjacent tie beams, and the two arrays of track foundation springs beneath the ties. To reduce the degrees of freedom involved in the track element, the resilient, flexural, and inertial effects of the substructure components are represented by an equivalent spring stiffness at each end of the rail span, as seen in Fig. 2.b. Thus, the generalized track element is simplified to a uniform rail beam segment supported at the two ends by two identical general spring coefficients $\hat{K}_e$. The equivalent spring coefficient depends on the elastic and inertial characteristics of the rail support components, as well as the vibration frequency, Ω, of the entire track. Its expression is given as follows:

$$\hat{K}_e = \frac{k_p}{1 + k_p \sum_{n=1}^{\infty} \frac{2[z_n(d_r)]^2}{(\omega_n^2 - \Omega^2)M_n}} \tag{1}$$

where k_p is the rail/tie contact stiffness; z_n is the n^{th} mode of the tie as an individual free beam on an elastic foundation; d_r is the length of tie outside the track gauge; ω_n is the undamped natural frequency of the individual free tie and; M_n is the corresponding generalized modal mass. The summation term in the denominator of the above relationship is in terms of either only symmetrical modes, or only asymmetrical modes. Eqn. (1) is derived (The procedure is omitted here) by applying the method of modal analysis to a rail substructure unit (see Fig. 2). This expression applies whether the tie is described by the Bernoulli–Euler theory, or by the Timoshenko theory. Note that system damping is ignored for the natural vibration analysis.

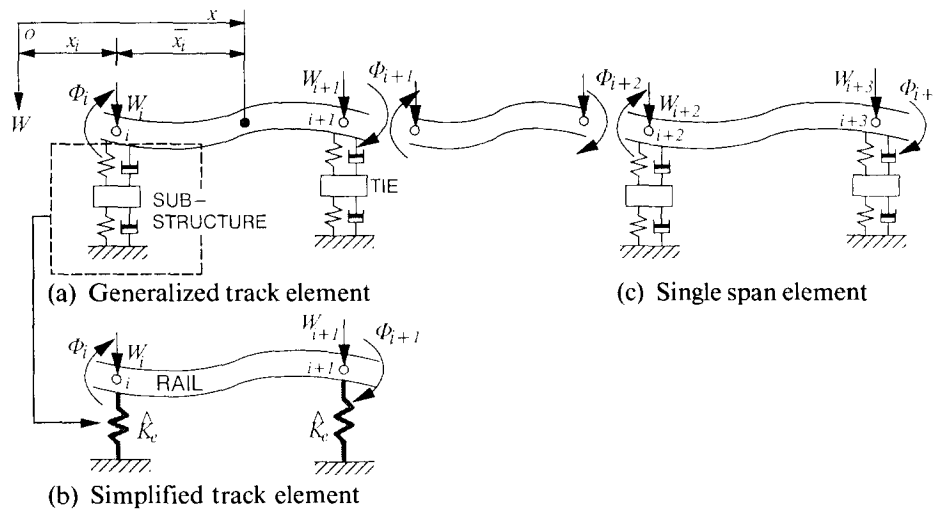

(a) Generalized track element

(c) Single span element

(b) Simplified track element

Fig. 2 Formulation of Generalized Track Element

Combining the above defined spring coefficient with the exact dynamic stiffness matrix (EDSM) of the rail span, the dynamic stiffness matrix of the generalized track element is formulated:

$$[K_r] = \begin{bmatrix} k_{11} + \hat{K}_e & k_{12} & k_{13} & k_{14} \\ k_{21} & k_{22} & k_{23} & k_{24} \\ k_{31} & k_{32} & k_{33} + \hat{K}_e & k_{34} \\ k_{41} & k_{42} & k_{43} & k_{44} \end{bmatrix} \tag{2}$$

Each element k_{ij} is a transcendental function of the undamped frequency Ω of the track. The expressions of k_{ij} are well documented in the literature for both the Bernoulli–Euler beam (Paz 1985) and the Timoshenko beam (Chen 1987, Capron and Williams 1988).

Thus, the entire track structure is idealized to a continuous assembly of the generalized track element and the adjacent single rail span element (Fig. 2.c) in a periodic manner.

3.2. Determination of natural frequencies and nodal displacements

The natural frequencies and vibrational modes of the track are determined by formulating its overall dynamic stiffness matrix. The system characteristic eigenfunction of the track then becomes:

$$| K_R (\Omega) | = 0 \tag{3}$$

where $[K_R (\Omega)]$ represents the global dynamic stiffness matrix, which is an assembly of the dynamic stiffness matrices of the generalized track elements (Fig. 2.b) and the single beam elements (Fig. 2.c). Obviously, only a limited extension of the track can be taken when formulating the global matrix $[K_R (\Omega)]$. The solution procedure of Eqn. (3) follows an algorithm similar to that developed by Wittrick and Williams (1971) and Williams and Kennedy (1988).

The n^{th} solution, Ω_n, of Eqn. (3) is now substituted into the following singular equation:

$$[K_R (\Omega_n)] \{\Delta_{Rn}\} = 0 \tag{4}$$

to obtain the eigenvector of the n^{th} mode, i.e., $\{\Delta_{Rn}\} = [W_{1n}, \Phi_{1n}, W_{2n}, \Phi_{2n}, \cdots, W_{Nn}, \Phi_{Nn}]^T$, where subscript N is the total number of ties accounted for in formulating $[K_R(\Omega)]$. The non-trivial solution of Eqn. (4) is achieved by using the Gaussian elimination method (with maximum pivoting), with the assignment of unity rotation angle to any arbitrary node (except the two end nodes and the center node).

3.3. Natural modes of rail

Once the i^{th} subvector of $\{\Delta_{Rn}\}$, i.e., $\{\Delta_{Rn}\}_i = [W_{in}, \Phi_{in}, W_{i+1,n}, \Phi_{i+1,n}]^T$, is determined, the mode shape function of the i^{th} rail span is obtained by solving the following ordinary differential equations that govern the natural vibration of the i^{th} rail beam segment, with $\{\Delta_{Rn}\}_i = [W_{in}, \Phi_{in}, W_{i+1,n}, \Phi_{i+1,n}]^T$ applied as the boundary condition at the two end nodes.

If the rail is described by the Bernoulli–Euler beam theory:

$$W_n^{(4)}(x) + \left(\frac{P_a}{EI_r} \right) W_n''(x) - \left(\frac{m_r \Omega_n^2}{EI_r} \right) W_n (x) = 0 \tag{5}$$

If the rail is described by the Timoshenko beam theory:

$$W_n''(x) + \left(\frac{m_r \Omega_n^2}{EI_r} \right) W_n(x) - \Phi_n (x) = 0 \tag{6.a}$$

$$\Phi_n''(x) + \left(\frac{m_r r_r^2 \Omega_n^2 - \kappa AG_r + P_a}{EI_r} \right) \Phi_n (x) + \left(\frac{\kappa AG_r}{EI_r} \right) W_n'(x) = 0 \tag{6.b}$$

where $W_n(x)$, $\Phi_n(x)$ are the n^{th} modal deflection and rotation angle of the rail; EI_r is the flexural rigidity; κAG_r is the shear rigidity (where k is the Timoshenko shear coefficient), m_r is the mass per unit length of rail; r_r is the radius of gyration of the rail beam cross-section and; P_a is the axial force existing in the rail. Solutions of the modal shape functions, $W_n(x)$ and $\Phi_n (x)$, from the above equations have been given by Chen (1987).

3.4. Natural modes of tie

Having determined from Eqn. (4) the nodal deflection of the rail, W_{in}, atop the i^{th} tie, the corresponding rail/tie contact force (or rail seat force), $f_{in}(t)$, may be expressed as:

$$f_{in}(t) = \hat{K}_{en} W_{in} e^{j\Omega_n t} \tag{7}$$

where $\hat{K}_{en}$ is the equivalent frequency-dependent spring coefficient corresponding to the n^{th} mode of the track. This force is then applied on the substructure unit to obtain the tie mode shape function:

$$Z_{in}(y) = \hat{K}_{en} W_{in} \sum_{m=1}^{\infty} \frac{2 z_m(y) z_m(d_r)}{M_m(\omega_m^2 - \Omega_n^2)} \tag{8.a}$$

$$\Psi_{in}(y) = \hat{K}_{en} W_{in} \sum_{m=1}^{\infty} \frac{2 \beta_m(y) z_m(d_r)}{M_m(\omega_m^2 - \Omega_n^2)} \tag{8.b}$$

where $Z_{in}(y)$, $\Psi_{in}(y)$ are the n^{th} modal deflection and rotation angle of the i^{th} tie in the track; $z_m(y)$, $\beta_m(y)$ are the deflection and rotation angle of the m^{th} mode of the tie as an individual free beam on an elastic foundation; M_m is the generalized mass of the m^{th} free tie mode and; ω_m is the corresponding m^{th} circular frequency. Eqn. (8) applies to both the Bernoulli–Euler beam and the Timoshenko beam.

4. Forced vibration of track/beam system

4.1. General equations of motion

Fig. 3 shows the segregated force diagram of the track/beam system model. The rail is loaded by a series of forcing functions represented by, $P_j(t)$, $j = 1,2,3,\cdots,J$, and the counteracting rail/tie contact forces, $f_i(t) = 1,2,3,\cdots,N$. The forces acting on a tie includes the two rail/tie interactive forces at the two rail seats and the distributed foundation reaction force $k_s z(y,t)$ per unit length of tie. Applying the Timoshenko beam theory to both the rail and the tie beams, the equations of motion for the track/beam system are derived:

1. For the rail,

$$\frac{\partial}{\partial x}\left\{ \kappa AG_r \left[\phi(x,t) - \frac{\partial w(x,t)}{\partial x} \right] \right\} + m_r \frac{\partial^2 w(x,t)}{\partial t^2} = -\sum_{i=1}^{N} f_i(t)\delta(x - il_p) + \sum_{j=1}^{J} P_j(t)\delta(x - x_j) \tag{9.a}$$

$$EI_r \frac{\partial^2 \phi(x,t)}{\partial x^2} - \kappa AG_r \left[\phi(x,t) - \frac{\partial w_i(x,t)}{\partial x} \right] - m_r r_r^2 \frac{\partial^2 \phi(x,t)}{\partial t^2} + P_a \phi(x,t) = 0 \tag{9.b}$$

where $w(x,t)$, $\phi(x,t)$ represent the rail deflection and rotation angle; $f_i(t)$, $P_j(t)$ represent the rail/tie interactive force and the forcing function on the rail; l_p is the tie spacing; x_j is the

x coordinate at which $P_j(t)$ is applied; and $\delta(x)$ is the Dirac delta function. For other denotations see Eqn. (6).

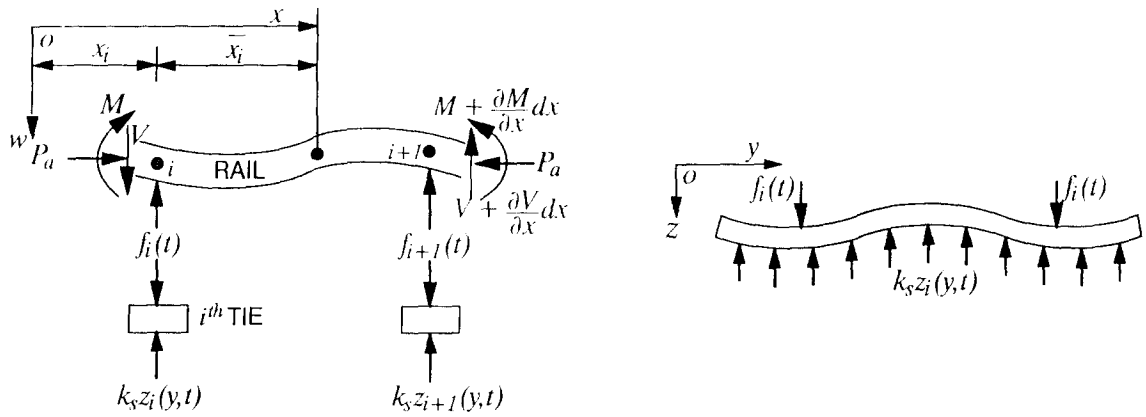

(a) Longitudinal view (b) Transverse view(i^{th} TIE)

Fig. 3 Schematic Force Diagram of Rail/Tie Beam System

2. For the i^{th} tie,

$$\frac{\partial}{\partial y}\left\{\kappa AG_t\left[\psi_i(y,t)-\frac{\partial z_i(y,t)}{\partial y}\right]\right\}+m_t\frac{\partial^2 z_i(y,t)}{\partial t^2}+c_s\frac{\partial z_i(y,t)}{\partial t}+k_s z_i(y,t)$$
$$=f_i(t)[\delta(y-d_r)+\delta(y-d+d_r)] \tag{10.a}$$

$$\frac{\partial}{\partial y}\left[EI_t\frac{\partial\psi_i(y,t)}{\partial y}\right]-\kappa AG_t\left[\psi_i(y,t)-\frac{\partial z_i(y,t)}{\partial y}\right]-m_t r_r^2\frac{\partial^2\psi_i(y,t)}{\partial t^2}=0 \tag{10.b}$$

where $z_i(y,t)$, $\psi_i(y,t)$ represent the deflection and rotation angle of the i^{th} tie; k_s, c_s are the distributed foundation stiffness and damping; EI_t, κAG_t are the flexural rigidity and the shear rigidity of the tie beam, respectively; m_t is the mass per unit length of tie; r_t is the radius of gyration of the tie beam; d is the total length of the tie; and d_r is the length of tie outside the track gauge. The equations of motion of the track are simpler when the Bernoulli–Euler beam theory is used and are omitted herein.

The compatibility condition for the above rail and tie equations of motion is achieved through the rail/tie interactive force:

$$f_i(t)=k_p[w(il_p,t)-z_i(d_r,t)]+c_p[\dot{w}(il_p,t)-\dot{z}_i(d_r,t)] \tag{11}$$

where k_p and c_p are the stiffness and damping coefficients of the rail/tie contact spring element.

4.2. Modal solutions

The solutions to the above partial differential equations of motion are expressed by the following modal transformation:

$$w(x,t)=\sum_{n=1}^{\infty} W_n(x)Q_n(t), \qquad \phi(x,t)=\sum_{n=1}^{\infty} \Phi(x,t)Q_n(t) \tag{12.a}$$

$$z_i(y,t)=\sum_{n=1}^{\infty} Z_{in}(y)Q_n(t), \qquad \psi_i(y,t)=\sum_{n=1}^{\infty} \Psi_{in}(y)Q_n(t) \tag{12.b}$$

Substituting Eqn. (12.a) into Eqn. (9), and Eqn. (12.b) into Eqn. (10), and performing an integration procedure over the track length l for the rail, and over the tie length d for all the N ties in the model, results in the following relationship for the modal time coefficient $Q_n(t)$:

$$\ddot{Q}_n(t)+\sum_{k=1}^{K} 2\xi_{nk}\Omega_n\dot{Q}_k(t)+\Omega_n^2 Q_n(t)=\bar{f}_n(t), \qquad (n=1,2,3,\cdots,K) \tag{13}$$

where K= number of modal terms truncated in Eqn. (12); Ω_n= angular frequency of the n^{th} mode of the track; ξ_{nk}=coupled modal damping ratio (mode n and k); and $\bar{f}_n(t)$=generalized modal force of the n^{th} mode.

The damping term ξ_{nk} is defined by:

$$\xi_{nk}=\frac{C_{nk}}{2M_n\Omega_n} \tag{14}$$

where M_n is the generalized modal mass of half the track/beam system (divided from the longitudinal centerline of the track) and is found from the orthogonality relationship between the mode shape functions of the rail and tie beams:

$$\int_0^l m_r[W_m(x)W_n(x)+r_r^2\Phi_m(x)\,\Phi_n(x)]dx+\sum_{i=1}^{N}\int_0^{d/2} m_t[Z_{im}(y)Z_{in}(y)+r_t^2\Psi_{im}(y)\Psi_{in}(y)]dy$$
$$=\begin{cases}0 & (m\neq n)\\ M_n & (m=n)\end{cases} \tag{15}$$

C_{nk} in Eqn. (14) is the coupled, or non-proportional, modal damping coefficient which can be calculated from:

$$C_{nk}=\sum_{i=1}^{N}\left\{c_p[W_n(il_p)-Z_{in}(d_r)][W_k(il_p)-Z_{ik}(d_r)]+\int_0^{d/2} c_s Z_{in}(y)Z_{ik}(y)dy\right\} \tag{16}$$

The generalized modal force $\bar{f}_n(t)$ of Eqn. (13) is expressed by the following equation:

$$\bar{f}_n(t)=\frac{1}{M_n}\sum_{j=1}^{J} W_n(x_j)P_j(t) \tag{17}$$

Eqn. (13) can be rewritten in the following standard matrix form by letting $Q_{n1}(t)=Q_n(t)$ and $Q_{n2}(t)=\dot{Q}_n(t)$:

$$\begin{Bmatrix}\dot{Q}_{n1}(t)\\ \dot{Q}_{n2}(t)\end{Bmatrix}=\begin{bmatrix}[0] & [I]\\ -[\Omega_n^2] & -2[\Omega_n][\xi_{nk}]\end{bmatrix}\begin{Bmatrix}Q_{n1}(t)\\ Q_{n2}(t)\end{Bmatrix}+\begin{Bmatrix}0\\ \bar{f}_n(t)\end{Bmatrix} \tag{18}$$

where $[\Omega_n^2]$ and $[\Omega_n]$ are diagonal matrices of size K with the diagonal elements being Ω_n^2 and $\Omega_n (n=1,2,3,\cdots,K)$, respectively; $Q_{n1}(t)=[Q_{11}(t), Q_{21}(t), \cdots, Q_{K1}(t)]^T$; $Q_{n2}(t)=[Q_{12}(t), Q_{22}(t), \cdots, Q_{K2}(t)]^T$; and $\bar{f}_n(t)=[\bar{f}_1(t), \bar{f}_2(t), \cdots, \bar{f}_K(t)]^T$; The damping matrix $[\xi_{nk}]$ is a full matrix:

$$[\xi_{nk}] = \begin{bmatrix} \xi_{11} & \xi_{12} & \cdots & \xi_{K1} \\ \xi_{21} & \xi_{22} & \cdots & \xi_{K2} \\ \vdots & \vdots & & \vdots \\ \xi_{K1} & \xi_{K2} & \cdots & \xi_{KK} \end{bmatrix} \tag{19}$$

where ξ_{ij} is determined from Eqn. (14). Thus, knowing the modal parameters of the track/beam system and the applied forcing functions, Eqn. (18) can be solved by any appropriate numerical routine. In this study, the 4-th order Runge-Kutta method with both fixed and adaptive time step is implemented. The forcing function $P_j(t)$ needs to be provided at discrete time intervals if no specific form of force-time relationship is given.

5. Example application of model to a typical track

As a numerical example to demonstrate the application of the vertical dynamic track model, the dynamic responses of a typical concrete-tie track subjected to a single wheel/rail impact force are presented herein. The forcing function is represented by a triangular force-time history (300 kN in magnitude and 2 ms in duration) shown in Fig. 4a, which is an approximate representation of an isolated wheel force impulse shown in Fig. 4b, measured under a wheelflat striking the rail. The parameters used for the track are given in Table 1.

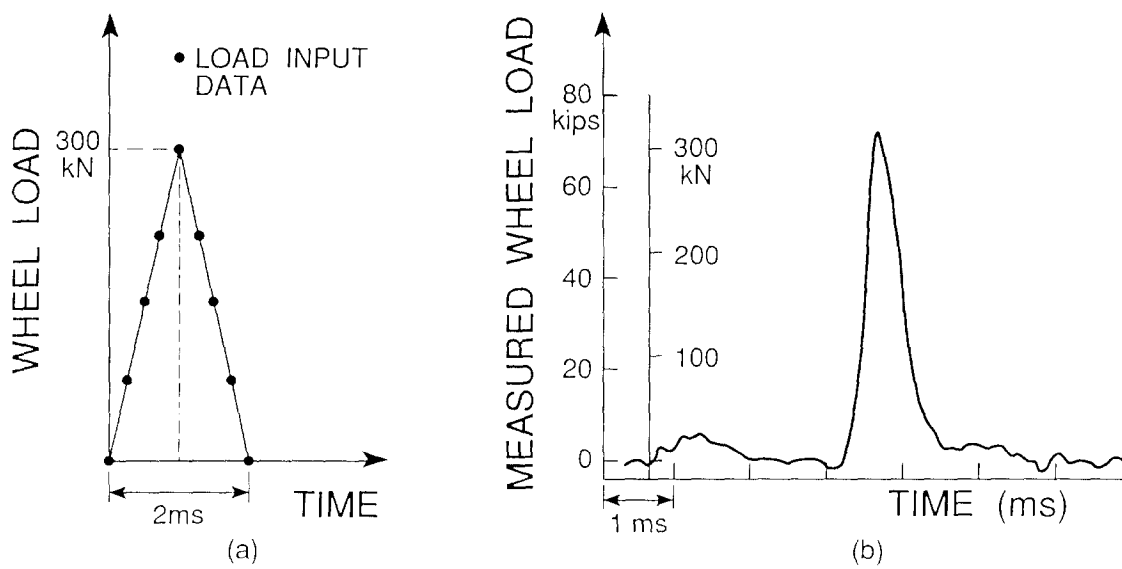

(a) Triangular Impact History Used as Input (b) Measured Wheel/Rail Impact Force

Fig. 4 Impact Force History

Table 1 Track Parameters

Rail and other track parameters	Tie Parameters
Elastic modulus $E_r = 207GN/m^2$	Elastic modulus $E_t = 70GN/m^2$
Poisson's ratio = 0.28	Poisson's ratio = 0.30
Timoshenko shear coeft. = 0.34	Timoshenko shear coeft. = 0.833
Cross-sectional area = $7.17 \times 10^{-3} m^2$	Tie spacing = $0.7m$
Second moment of area = $23.5 \times 10^{-6} m^4$	Tie length = $2.50m$
Radius of gyration = $57.2 \times 10^{-3} m$	Tie width = $0.25m$
Bending rigidity $EI_r = 4.86MNm^2$	Depth of mid section = $0.14m$
Shear rigidity $kAG_r = 197.2MN$	Depth of shoulder section = $0.21m$
Unit mass $m_r = 56.3kg/m$	Rail gauge length = $1.50m$
	Tie end to rail seat = $0.50m$
Rail pad stiffness $k_p = 280MN/m$	
Rail pad damping $c_p = 63000Nsm^{-1}$	
Track bed stiffness $k_s = 144MN/m/m$	
Track bed damping $c_s = 65600Nsm^{-2}$	
Axial force $P_a = 0$	

The frequencies obtained from Eqn. (3) for the case of Timoshenko type rail and tie, with different number of ties are listed in Table 2 for a variety of selected natural modes. It is seen that when the number of ties reaches 20, the variation in the natural frequency of the track becomes insignificant. All further calculations are then performed using a 25-tie length track model. The use of a finite extension model to solve both dynamic and static loading problems or rail tracks has also been reported by others (Nielsen and Abrahamsson 1992, Clark et al. 1982, Newton and Clark 1979/El-Ghazaly et al. 1991).

Table 2 Frequencies (Hz) of Selected Modes Obtained with Different Number of Ties (Timoshenko Rail and Tie Beams)

Mode No. / No. of Ties	1	10	30	50	70
5	161.3	250.8	767.3		
10	158.6	222.4	551.4	1100.	
15	158.4	186.5	442.0	865.1	1155.
18	158.4	182.9	260.2	534.6	902.2
20	158.3	176.1	251.5	446.8	789.6
25	158.3	176.0	250.0	443.4	783.2
30	158.3	176.0	249.2	440.3	780.5

5.1. *Deflection and acceleration responses of rail*

Fig. 5a and 5b show the deflection and acceleration responses of the rail at different loca-

tions in relation to the impact force. The corresponding static rail deflections calculated according to the AREA recommended procedure are also given in Fig. 5a using a peak impact force of 300 kN. It is seen that the static deflection of the rail calculated in such a way is generally larger than the peak dynamic deflection. For the acceleration response of the rail, the peak acceleration at each midspan position is greater than those above the two neighboring ties. This pattern of acceleration response shows the effect of considering the rail substructure system as discrete supports.

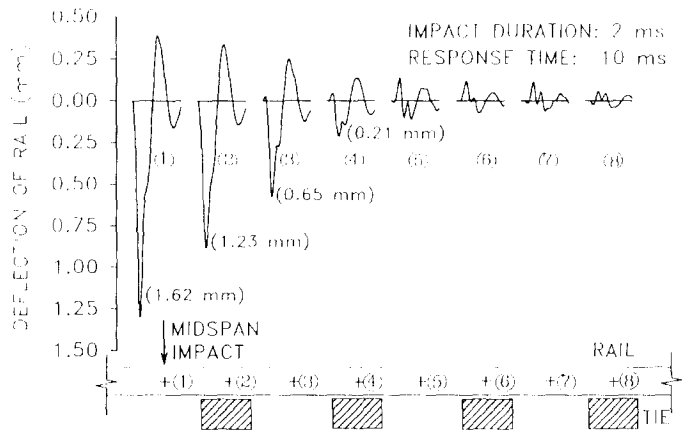

(a) Rail Deflection

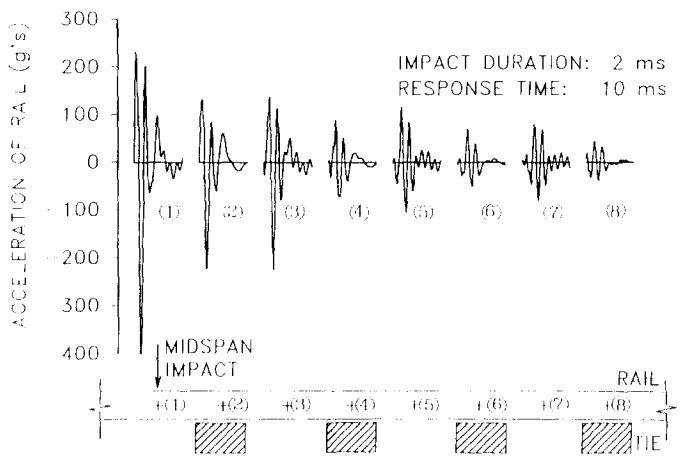

(b) Rail Acceleration

Fig. 5 Time Histories of Rail Deflection and Acceleration Response along the Track

5.2. Normal and shear stress/strain responses of rail

The time histories of the dynamic normal stress/strain at the top of the rail head, and the shear stress/strain along the rail neutral axis, are shown in Fig. 6a and 6b, respectively. The normal stress/strain is dominantly compressive under the impact point within the 2 ms duration of impact. Tensile stress/strain starts to become more prominent from the second span.

In fact the maximum dynamic peak tensile response occurs within the second span, and does not decrease noticeably until the third span from the impact. One implication from this dynamic behavior is that, if there exists a transverse defect in the rail head, such as an internal crack, the critical condition (for brittle rail breakage) occurs when the impact force is some distance away from the defect.

A comparison between the dynamic peak stresses and the static results (numerical values) in Fig. 6a shows that the largest difference occurs at the first midspan from the impact, location (3), where tensile stress dominates. At this point the dynamic stress is over 70% higher than the static stress. The maximum static tensile stress occurs at location (4) above the second tie from the impact. This maximum static stress is still over 40% lower than the peak dynamic stress at location (3). Such a marked difference in the predicted dynamic and static tensile stress responses has significant implications for the evaluation of the rail's susceptibility to wheel impact when there exist internal transverse defects in the rail head. Clearly, the static analysis will considerably underestimate the destructive tensile stresses caused by a wheel impact.

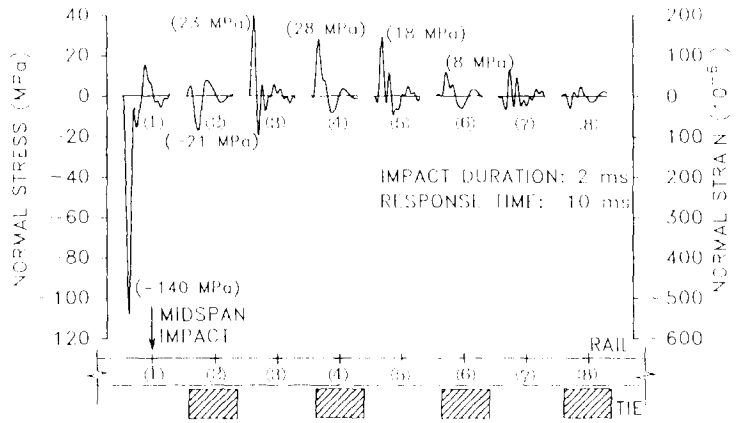

(a) Normal Stress/Strain at Rail Head

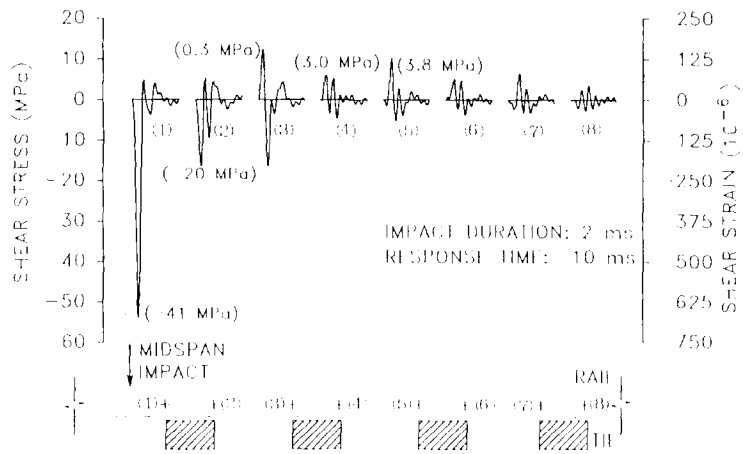

(b) Shear Stress/Strain along Rail Neutral Axis

Fig. 6 Time Histories of Rail Normal and Shear Stress/Strain Response along the Track

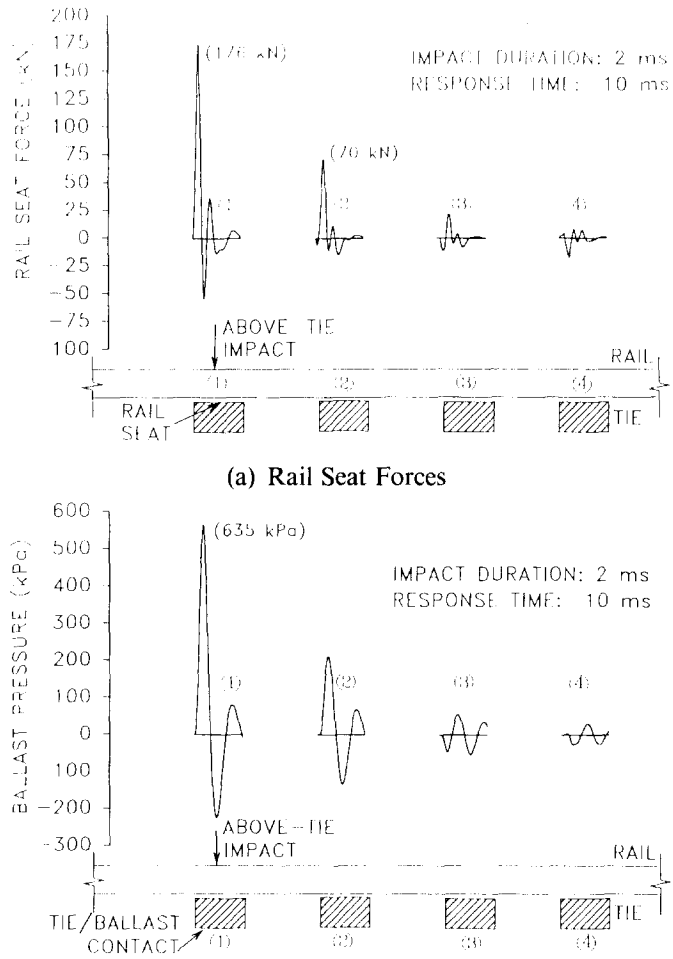

(a) Rail Seat Forces

(b) Ballast Pressure

Fig. 7 Time Histories of Rail Seat Force and Ballast Pressure Response along the Track

Unlike the normal stress/strain response, that is calculated at the top of the rail head, the dynamic shear response (Fig. 6b) is obtained at the neutral axis of rail cross-sections close to the tie edges. Comparing the shear response and the normal response, it is seen that the peak shear stress of the first cross-section is nearly 50% of the normal stress at the midspan impact point. The corresponding shear and normal strains at other locations along the rail are also very significant as compared to the normal stress/strain responses. This indicates that dynamic shear stresses cannot be neglected in calculating track responses under impact loading, as is the case under static conditions.

5.3. Rail seat force and ballast pressure responses

The rail seat force and ballast pressure responses as shown in Fig. 7 illustrate a rapid decrease in the rail/tie interaction away from the impact position. The rail seat force immediately below the impact is 55% of the peak magnitude (300 kN) of the applied triangular forcing

function. The rail seat force on the tie adjacent the impact position is approximately 25% of the impact peak, and that on the next tie is less than 10% of the impact peak. As shown in Fig. 7a, the static analysis using the AREA recommended procedure results in very close rail seat forces to the dynamic predictions for the first two ties. The ballast pressure responses (The track foundation spring is assumed to be capable of taking tension) in Fig. 7b show the same trend of variation as the rail seat forces. But the dynamic magnitude is smaller than the static result.

5.4. *Rail/tie deflected shapes and spatial distributions of dynamic stresses/strains*

For the same triangular impact, the deflected shapes of the rail at different time increments and the corresponding normal stress variations at the top of the rail head are shown in Fig. 8a and Fig. 8b, respectively. The static results under the pseudo-dynamic load (300 kN) are also shown. It is interesting to observe that rail rebounding immediately below the impact point starts occurring at approximately 1.5 ms which is before the duration of the impact forcing function. The travelling deflection wave is clearly demonstrated by the deflected shapes of the rail at 1.5 and 2 ms. It is seen that the rail portion within the first tie is rebounding, while the rail beyond the first tie is still deflecting downward.

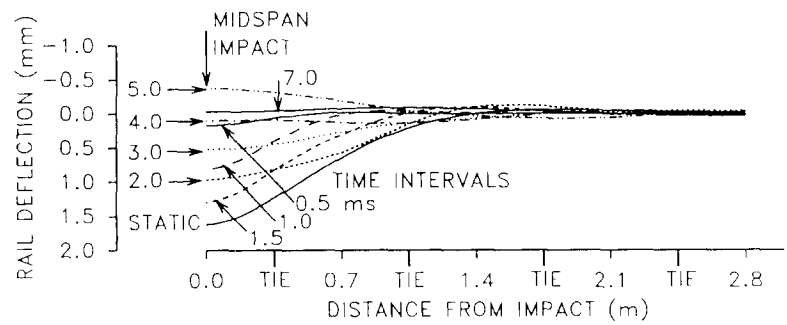

(a) Rail Deflection

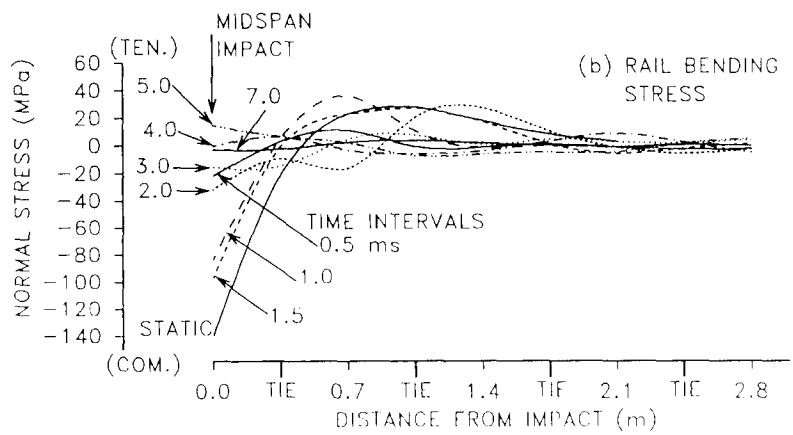

(b) Rail Bending Stress at Rail Head

Fig. 8 Rail Deflected Shapes and Normal Stress Distributions at Different Time Intervals

The variations pattern of rail head stresses at different time intervals shown in Fig. 8b facilitates Fig. 6a in identifying the region of compressive and tensile stresses along the rail head (or rail base). From the stress wave curves at 1.0, 1.5 and 2.0 ms it can be seen that dominantly tensile stresses occur within a region from the first to the third tie away from the impact point. Of course the maximum compressive stress occurs directly under the impact load. Beyond the third tie, the rail head stresses, both compressive and tensile, die away rapidly due to both the system stiffness and damping effect of the track.

The deflection and the top-fiber normal stress distribution curves of the tie at different time intervals are shown in Fig. 9a and Fig. 9b. The corresponding static curves are also given. Two values of the elastic modulus of the tie are used for the static analysis, one is the "dynamic" value of 70 GN/m^2 as listed in Table 1, the other is the static value of 35 GN/m^2. The plots indicate that the magnitude of the tie's elastic modulus does not have any significant effect on the static deflection of the tie. Its effect on the static normal stress of the tie within the rail seat region is also negligible. Appreciable effect on the static stress distribution occurs within the tie center region. As expected, compressive stresses dominate the rail seat area, and tensile stresses dominate the tie center area. The reverse is true for stress responses along the bottom fiber of the tie beam.

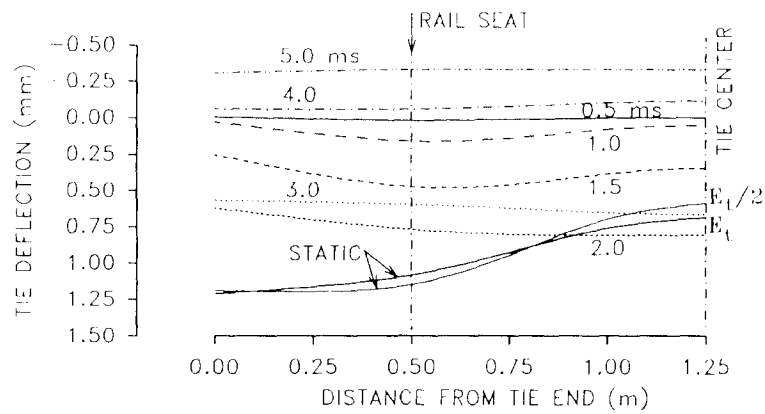

(a) Tie Deflection

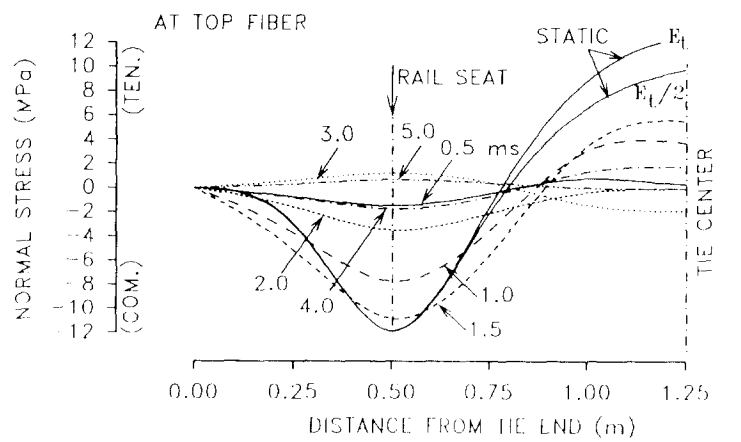

(b) Tie Bending Stress at Top Fiber

Fig. 9 Tie Deflected Shapes and Normal Stress Distribution at Different Time Intervals

It is observed that the vertical movement of the tie involves both rigid body motion and transverse flexure, with the former being dominant (Fig. 9a). The degree of bending increases as the tie moves down, as illustrated by the deflection curves at 0.5, 1.0 and 1.5 ms, and the corresponding bending stress distributions (Fig. 9b). The degree of bending decreases as the tie moves further down until it reaches the maximum deflection at 2.0 ms. Less bending component is seen during the rebounding.

5.5. *Comparison between solutions with Timoshenko and Bernoulli–Euler beam theories*

In the previous examples, the Timoshenko beam theory is chosen to represent the rail/tie beams. To demonstrate how the rotatory inertia and shear distortion of the rail/tie beams considered in the Timoshenko beam theory affect the dynamic behavior of the track, representative solutions of track responses under the impact point are obtained with the Bernoulli–Euler theory being applied to describe the rail and tie beams. The results are compared with the corresponding solutions when the Timoshenko theory is used. Space limitations do not permit full diagrammatic comparisons, however, the following general findings are made.

Except for the tie deflection, the above–tie normal stress/strain of the rail, and the ballast pressure responses, there exist appreciable differences between the two sets of solutions. The differences are most apparent within the duration of the impact forcing function, especially at the peak responses. It is always the use of the Timoshenko theory that yields higher magnitudes of the calculated responses. This clearly indicates that the rotatory inertia and the shear distortion considered in the Timoshenko beam theory are significant factors affecting the dynamic behaviors of the track/beam system under sharp impact loading and should not be neglected in studying rail track dynamics. The use of the Bernoulli–Euler theory to describe the rail and tie beams may underestimate the effects of wheel/rail impact loading.

6. Conclusion

A vertical dynamic rail track model that is capable of predicting dynamic track responses to any arbitrary loading function has been presented. The solution to the track dynamic responses has been made possible by the formulation of a generalized track element and the innovative concept of an equivalent frequency dependent spring coefficient superseding the general effects of the track substructure system. Dynamic solutions that are of particular interest to the track engineer, such as rail/tie deflections, stresses/strains, accelerations, rail seat forces, and ballast pressures caused by a given wheel/rail impact force history, can be readily obtained. By using a deterministic stationary impact function as an excitation source to the track system, valuable insight into the characteristics of rail track dynamic responses can be gained (The interpretation of a large scale drop–weight test by Igwemezie et al. 1993, using the presented model is currently under way; Other reported drop–weight test data is also being compiled to calibrate the model). Existing pseudo–static approaches (AREA 1991) to analyzing track responses under wheel/rail loads can also be evaluated.

Through a numerical example, the following fundamental characteristics of track responses are observed:

(1) The static analysis using a load equivalent to the peak of a dynamic forcing function results in conservative results for the rail/tie deflection and normal stress/strain responses

under the load point. But the static analysis considerably underestimates the tensile stresses in the rail head some distance away from the impact point (The same is true for compressive stresses in the rail base).
(2) The shear stresses and strains in the rail are considerably lower from the static analysis than from the dynamic analysis. The shear behavior of the rail should not be ignored in any dynamic analysis of the track.
(3) For this set of particular track parameters (Table 1), the static analysis results in rail seat forces that are very close to the predicted dynamic rail seat forces at the peak, but gives higher ballast pressure than the dynamic analysis.
(4) The vertical movement of the tie under impact comprises two components, the rigid body motion and the transverse bending. Within the top fiber of the tie beam, compressive stress dominates in the rail seat area while tensile stress dominates in the tie center region (The reverse is true for the stresses/strains within the bottom fiber of the tie beam).
(5) The rotatory inertia and the shear distortion considered in the Timoshenko beam theory are significant factors affecting the dynamic behavior of the track/beam system under impact loading and should not be neglected in studying rail track dynamics. The use of the Bernoulli–Euler theory to describe the rail/tie beams may considerably underestimate the effects of wheel/rail impact loading.

Acknowledgements

Acknowledged is funding to conduct this study from a National Scientific and Engineering Research Council (Canada) grant awarded to the authors.

References

Cai, Z. and Raymond, G.P. (1992), "Theoretical Model for Dynamic Wheel/Rail and Track Interaction", *Proc. 10th Int. Wheelset Congress,* Sydney, Australia, Sept., 1992, pp. 127–131.

Cannon, D.F. and Sharpe, K.A. (1981), "Wheel Flats and Rail Fracture", *Proc. Seminar Organized by BR R &D and AAR,* Nottingham, England, Sept. 21–26, 1981, pp. 163–177.

Capron, M.D. and Williams, F.W. (1988), "Exact Dynamic Stiffnesses for an Axially Loaded Timoshenko Member Embedded in an Elastic Medium", *J. Sound Vib.*, **124**, pp. 453–466.

Chen, Y.H. (1987), "General Dynamic Stiffness Matrix of a Timoshenko Beam for Transverse Vibrations", *Earthquake Eng. Struct. Dyn.*, **15**, pp. 391–402.

Clark, R.A., Dean, P.A., Elkins, J.A. and Newton, S.G. (1992), "An Investigation into the Dynamic Effects of Railway Vehicles Running on Corrugated Rails", *J. Mech. Eng. Sci.*, **24**, pp. 65–76.

Dean, F.E., Ahlbeck, D.R., Harrison, H.D. and Tuten, J.M. (1982), "Effect of Tie Pad Stiffness on the Impact Loading of Concrete Ties", *Proc. 2nd Int. Heavy Haul Railway Conf.*, Colorado Springs, USA, Paper 82 HH–41.

Duffy, D.G. (1990), "The Response of an Infinite Railroad Track to a Moving, Vibrating Mass", *J. App. Mech.*, ASME, **57**, pp. 66–73.

El-Ghazaly, H.A., Sherbourne, A.N. and Arbarbi, F. (1991), "Strength and Stability of Railway Tracks–II, Deterministic, Finite Element Stability Analysis", *Comp. Struct.*, **39**, pp. 23–45

Fryba, L. (1972), "Vibration of Solids and Structures under Moving Loads", Groningen: Noordhoff International Publishing.

Grassie, S.L. and Cox, S.J.(1984), "The Dynamic Response of Railway Track with Flexible Sleepers to High

Frequency Vertical Excitation", *Proc. Inst. Mech. Eng.*, 7, 198D, pp. 117–124.
Grassie, S.L. (1984), "Dynamic Modelling of Rail Track and Wheelsets", *Proc. 2nd Int. Conf. Recent Advances in Structural Dynamics*, University of Southampton, pp. 681–698.
Igwemezie, J., Kennedy, S. and Cai, Z. (1993), "Calibration of Railway Track for Dynamic Loads", *Transport Canada Report TP 11569E.*
Kenney Jr., J.T. (1954), "Steady State Vibrations of Beam on Elastic Foundation for Moving Load", *J. App. Mech.*, ASME, **76**, pp. 359–364.
Kerr, A.D. (1972), "The Continuously Supported Rail Subjected an Axial Force and a Moving Load", *Int. J. Mech. Sci.*, **14**, pp. 71–78.
Lewandowski, L. (1991), "Non-Linear, Steady-State Analysis of Multispan Beams by the Finite Element Method", *Comp. Struct.*, **39**, pp. 83–93.
Mead, D.J. and Yaman, Y. (1991), "The Response of Infinite Periodic Beams to Point Harmonic Forces: A Flexural Wave Analysis", *J. Sound Vib.*, **144**, pp. 507–530.
Munjal, ML. and Heckl, M. (1982), "Vibrations of a Periodical Rail-Sleeper System Excited by an Oscillating Stationary Transverse Force", *J. Sound Vib.*, **81**, pp. 491–500.
Nielsen, J.C.O. and Abrahamsson, T.J.S. (1992), "Coupling of Physical and Modal Components for Analysis of Moving Non-Linear Dynamic Systems on General Beam Structures", *Int. J. Num. Meth. Eng.*, **33**, pp. 1843–1859.
Newton, S.G. and Clark, R.A. (1979), "An Investigation into the Dynamic Effects on the Track of Wheelflats on Railway Vehicles", *J. Mech. Eng. Sci.*, **21**, pp. 287–297.
Ono, K. and Yamada, M. (1989), "Analysis of Railway Track Vibration", *J. Sound Vib.*, **130**, pp. 269–297.
Patil, S.P. (1988), "Response of Infinite Railroad Track to Vibrating Mass", *J. Eng. Mech., ASCE*, **114**, pp. 688–703.
Paz, M. (1985), *Structural Dynamics*, van Nostrand Reinhold Company Inc., Chapter 21.
Raymond, G.P. and Cai, Z. (1993), "Dynamic Track Support Loading from Heavier/Faster Train Sets", *Trans. Res. Rec.* 1381, National Research Council, Washington, D.C., pp. 53–59.
Scott, J.F. and Charenko, A. (1985), "Concrete Ties – Measurement of Rail Impact Forces from Stationary Drop Tests and Evaluation of Resilience of Rail Seat Pads", *Transport Canada Report TP 7352E.*
Wittrick, W.H. and Williams, F.W. (1971), "A General Algorithm for Computing Natural Frequencies of Elastic Structures", *Quart. J. Mech. App. Math.*, **24**, Part 3, pp. 263–284.
Williams, F.W. and Kennedy, D.(1988), "Reliable Use of Determinants to Solve Non-linear Structural Eigenvalue Problems Efficiently", *Int. J. Num. Meth. Eng.*, **26**, pp. 1825–1841.